Analysis of Radiation Patterns in Three-Phase Motor with the Stator Winding as a Circular Array of Antenna

Jeonghwan Kim

Department of Electrical Engineering

Graduate School of UNIST

Analysis of Radiation Patterns in Three-Phase Motor with the Stator Winding as a Circular Array of Antenna

A thesis
submitted to the Graduate School of UNIST
in partial fulfillment of the
requirements for the degree of
Master of Science

Jeonghwan Kim

06. 07. 2019
Approved by

_____

Advisor
Jingook Kim

Analysis of Radiation Patterns in Three-Phase Motor with the Stator Winding as a Circular Array of Antenna

Jeonghwan Kim

This certifies that the thesis of Jeonghwan Kim is approved.

06. 07. 2019

signature

_____

Advisor: Jingook Kim

signature

_____

Ki Jin Han: Thesis Committee Member #1

signature

_____

Gangil Byun: Thesis Committee Member #2

Abstract

This thesis presents method of estimating radiated emission (RE) occurring in stator winding of three-phase motor drive system. The stator winding of given reference motor model is assumed as circular array of radiating antennas. Radiation patterns can be obtained by calculation of magnetic vector potential of balanced three-phase current source distribution.

Analysis in far-field radiation region boundary instead of near-field radiation region is proceeded in the condition of the CISPR 25 standard. Radiation patterns are estimated in fixed measurement distance within various frequency band. Radiation region boundary classification is defined under the given frequency range. Far-field condition is essential progress to justify the proposed approach.

The radiation patterns can be estimated by 3D full-wave electromagnetic simulation using finite element method (FEM). Each radiation patterns can be calculated by analyzing both theta (θ) component and phi (ϕ) component. The fields are analyzed in case when $\theta = 90°$ and $\phi = 90°$. Radiated electric fields can be measured in every single degree.

The harmonic frequency that excites the far-field radiation can be any integer multiple of the fundamental line frequency. When the harmonic number is multiple of three, the radiated electric fields suppress each other due to the balanced current distribution. However, when harmonic number is not multiple of three, the current source involved in motor operation has appropriate sequence. The meaningful radiation patterns can be analyzed with the correctly involved three-phase current excitation.

The stator winding coils are closely positioned, mutual coupling effect among the coils cannot be neglected. The multi-port RLC network circuit model is proposed to compensate in order to calculate proper radiation patterns.

Loop of coil contains two axial and two end-turn current direction. Each magnetic vector potential can be obtained by summing each phase current density. The phi-directional electric field is origin by current distribution of end-winding component of current source. On the other hand, the theta-direction electric field is related to axial component. The analysis of radiation patterns represents the dominant radiation component in AC motor operation.

Contents

List of Figures

List of Tables

Nomenclature

EMI	Electromagnetic Interference
3D	Three Dimension
AC	Alternating Current
DC	Direct current
RE	Radiated Emission
RF	Radiofrequency
FEM	Finite Element Method
PCB	Printed Circuit Board

Chapter I

Introduction

High-tech designed applications of electric machines are constantly proposed in modern automotive industry. Noise coupling from complicated electronic devices cause degrade in reliability of overall system in systematic motor drive. Thus, electromagnetic interference (EMI) issue is always important factor to consider in design of the motor drive system [1][2].

Due to rapid development in modern technology, switching speed of power switches is getting faster and high-speed drive system, operating in radio frequency band, is frequently proposed. The design progress in this system recommend analysis of radiated emission (RE) as well as conducted emission (CE) [3][4]. Figure 1. illustrates radiated emission occuring in AC motor drive sysem.

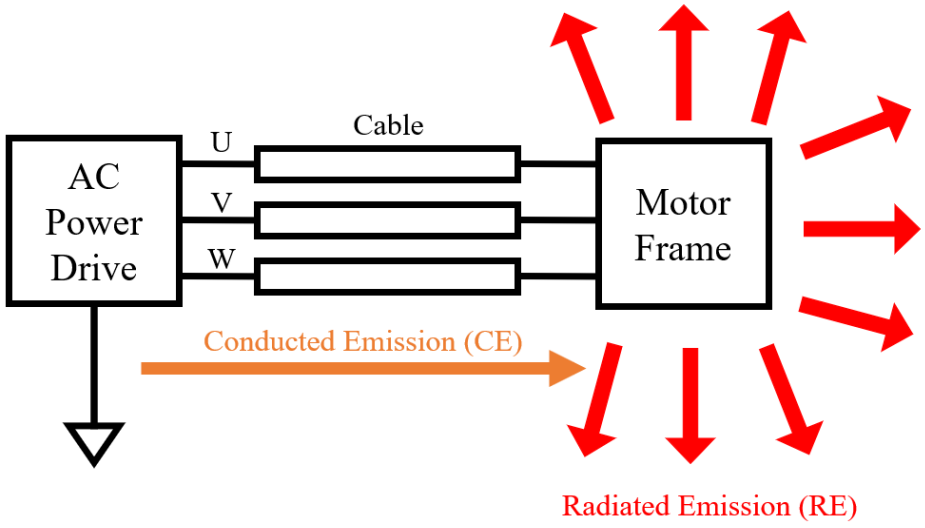

Figure 1. Noise coupling occurring in AC motor drive system

Various approaches to analyze radiated emission have been proposed in recent research. The issue of electromagnetic emissions from electrical rotating machinery is considered [5]. Approximated three-phase induction machine model is proposed to predict far-field radiation is proposed with PWM input [6]. Moreover, the 3D model using finite elements method (FEM) is also suggested to estimate electromagnetic field interference in motor drives [7]. Substitute method using disturbance currents and transfer functions are also proposed to calculate radiated emissions from drive system [8].

Analysis of RE from electric drive system has been frequently investigated. However, analysis of the radiation patterns in motor itself is not much presented. With the array antenna approach, realistic winding models are analyzed in this study to predict the radiated emission from stator windings of AC

motors.

Before measuring radiated emissions of AC motor, estimating radiation pattern by 3D simulation is essential progress. Realistic stator winding model is designed with practical operating motor parameters. With the model, 3D full-wave electromagnetic simulation can analysis S-parameters of realistic designed 3D model, as well as radiated electric fields in sweep of every angles.

An analytic approach to estimate radiation pattern can follow array antenna theory. Winding structure of three-phase AC motor can be considered as array of circular radiators. Single coil radiator consists of two axial components and two end-winding components excitations. Each spatial current distribution component can derive each magnetic vector potential to analyze radiation pattern. The comparison of radiation pattern measured in realistic winding model and estimation of calculation through array antenna method in the resonant frequency is eventual purpose.

Mutual coupling among coils cannot be ignored since coils are closely positioned without shielding. Multi-port RLC circuit model is suggested to resolve mutual coupling affection. The equivalent circuit model can be constructed by integral equation based on RLC extraction tool. The modified approach is expected to compensate discordance of radiation pattern due to unbalanced coupling.

Excited cases according to harmonic numbers must be classified to analyze radiation pattern in three-phase system. Generally, harmonic excitation maintains the original phase sequence or reversed. Electromagnetic analysis remains unaffected by order of phase excitation due to symmetry of winding structure. However, in case of zero harmonic factor excitation, all the phase excitations have the equal phase and the balanced current distribution of three-phase coils suppresses each other.

In chapter 2, winding structure and motor model including specific parameters are discussed. Reference model including winding structure is proposed in detail. Regions of the electromagnetic field around an object, whether to analyze in near-field or far-field is necessary to consider as well. Reference model is supposed to predict radiation pattern before measuring radiated emission from existed winding structure.

In chapter 3, analytic approach of array antenna model for motor EMC is described. In priority, the structure of stator winding poles is supposed as array of antenna. To estimate the radiation in antenna method, the approach of axial and end-winding component excited current is proceeded. Each magnetic vector potential component is derived mathematically and arranged in equation of phase current. Also, the mutual coupling of excited current is considered.

In chapter 4, the process of measurement in each step is described which is divided into several steps

in general. Firstly, PCB which separates input power into three different phases is designed to operate in RF band. And then, looped windings and motor model skeleton which can arrange array of winding appropriately is made to role as real operation motor. Every component is combined to measure radiation pattern in antenna chamber.

Chapter 2

Design of winding structure and estimation of radiated emission in reference motor model

In this chapter, design of reference motor including specific stator winding parameters are discussed. Proposed model consists simplest three-phase integral slot winding structure. Considering symmetric conditions, current linkage distributions, winding factors are key factor to analyze radiated emissions from stator winding.

To estimate radiation patterns from three-phase motor, far-field condition must be obtained since analytic approach is only suitable for far-field radiation. With the fixed distance, electrical size of radiator can be classified in frequency range. According to the standards of CISPR25 [9], measurement distance between radiator and receiver is fixed. Radiation region boundary classification in given condition is proceeded to find far-field condition.

2.1 Modeling of stator winding in three-phase motor

A three phase ac motor is composed of a rotor and a stator. In the stator, a three-phase armature winding is constructed to generate rotating magnetic fields. The rotor can include permanent magnets (for synchronous motors) or shorted conductors (for induction motors). As radiating sources in high frequencies over megahertz range, the stator winding structure is more dominant than the rotor due to the difference of penetration depth in the ferromagnetic cores. Furthermore, magnetic permeability of ferromagnetic core is that of vacuum. In other words, the magnetic core of stator can be neglected when analyzing electromagnetic compability of overall structure. Therefore, focusing on radiation occurring from excitation of stator winding neglecting both magnetization of rotor and stator is proper method to measure radiation in AC motor system [6].

The armature winding of a three-phase electrical machine is constructed in the stator. Figure 2. shows the structure of single layer three-phase integral slot stator winding. Design parameters are arranged in Table 1. For non-fractional slot winding structure, the higher value of q makes more sinusoidal current linkage of the stator winding. Proposed model has doubled number of slots per pole and phase compared to simplest non-fractional three-phase slot winding. Figure 3. illustrates linear winding sequence of stator winding including single port excitation direction.

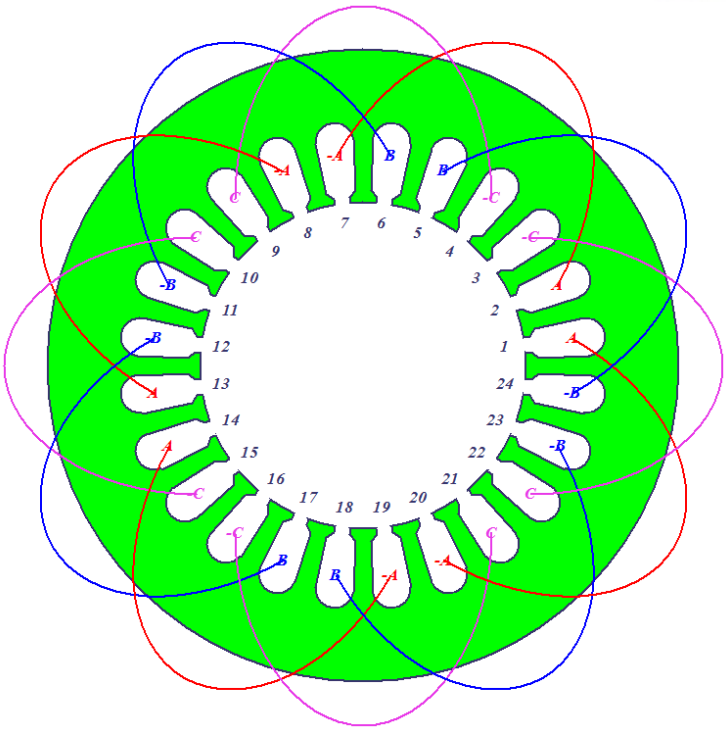

Figure 2. Winding diagram of proposed model

Table 1. Specific parameters of proposed model

Parameters	Value
Slot number, Q	24
Pole number (Pole pairs, p)	4(2)
Phase, m	3
Number of slots per pole and phase, q	2
Pole pitch	6
Turn number	12
Port excitation [W]	1
Axial coil length [mm]	210
Stator diameter [mm]	290

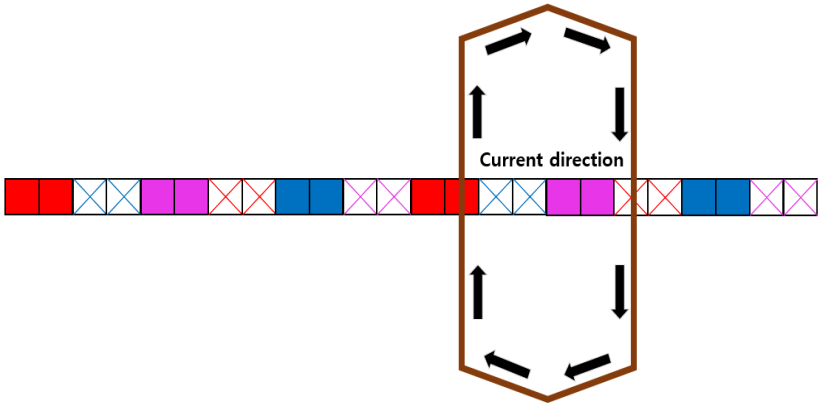

Figure 3. Winding sequence and current direction excited in single port

Winding structure must satisfy two symmetric conditions [10].

(a) The number of coils per phase winding must be integer. ($\frac{Q}{2m} = pq \in \mathrm{N}$)

(b) The angle between the phase winding (α_{ph}) must be an integer multiple of the angle phasor angle (α_z), where t stands for largest common divider of Q and p. ($\frac{\alpha_{ph}}{\alpha_z} = \frac{Q}{mt} \in \mathrm{N}$)

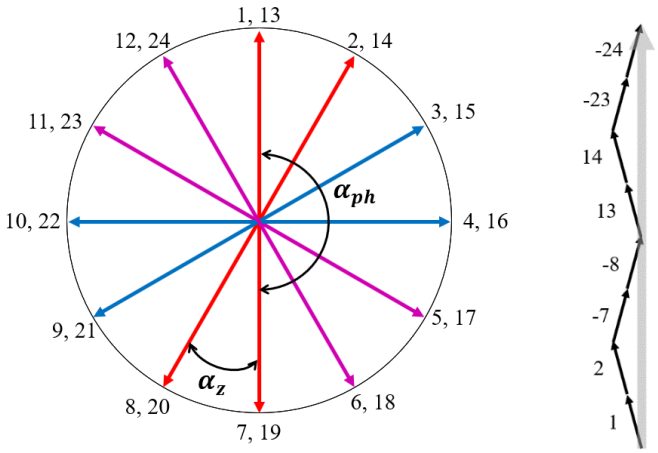

Figure 4. Voltage phasor diagram of a four-pole and three-phase winding

The stator winding contains 24 slots including three phases with four poles. 8 slots are excited with single phase. Fundamental voltage phasor diagram for the winding and calculation of the voltage in a single phase are illustrated in Figure 4. Winding factor (k_{w1}) based on the distribution of the winding for the fundamental can be calculated as a ratio of geometric sum and sum of absolute values.

$$k_{w1} = \frac{\text{geometric sum}}{\text{sum of absolute values}} = \frac{U_1 + U_2 - U_7 - U_8 + U_{13} + U_{14} - U_{19} - U_{20}}{|U_1| + |U_2| + |U_7| + |U_8| + |U_{13}| + |U_{14}| + |U_{19}| + |U_{20}|} = 0.966$$

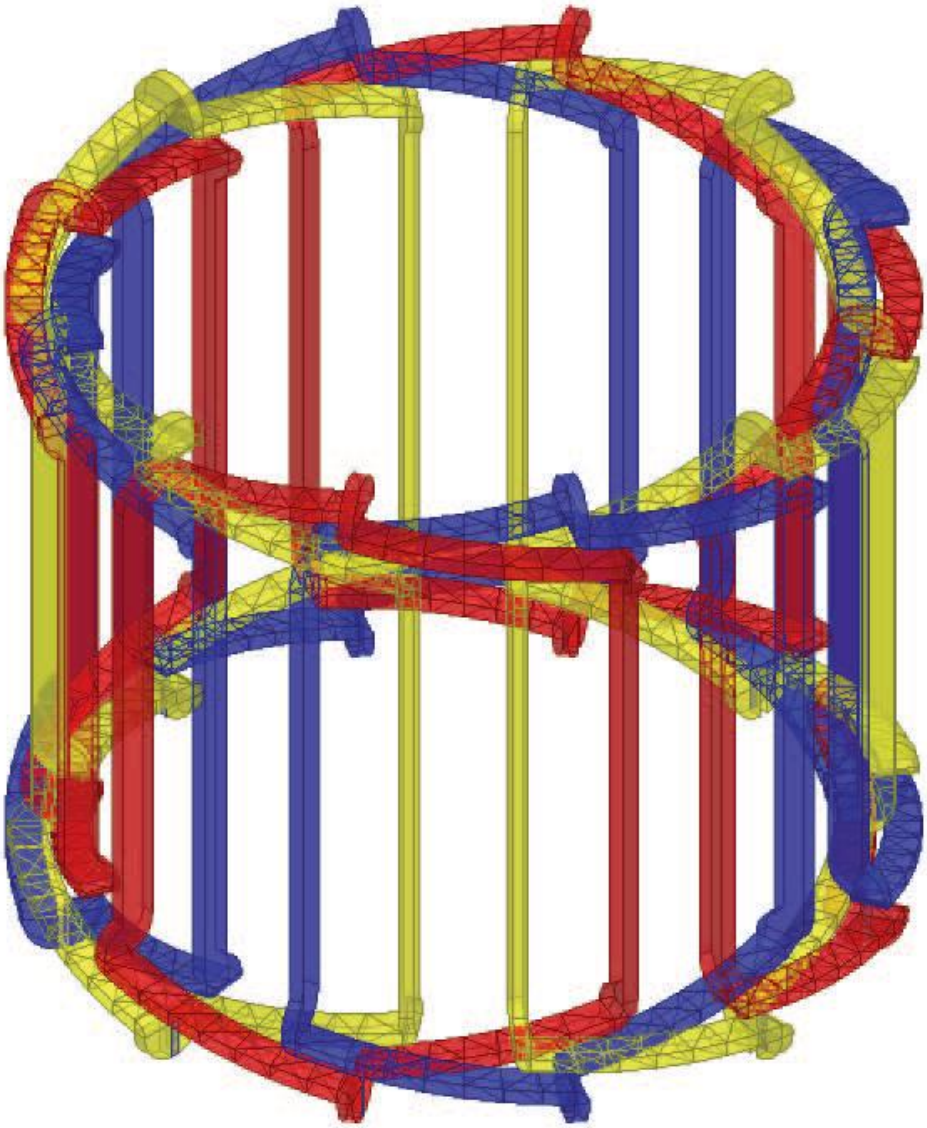

Figure 5. Simulation model of stator winding

Figure 5. illustrates stator winding structure including distinction of three phases. The structure is designed using RMXPRT. As discussed in the first paragraph, simulation model is composed of single stator winding without stator and rotor cores. U, V, W phases are labeled in different colors with appropriate sequence. Every phase is involved with 1W of port excitation with 120° differences. One loop of stator winding contains two slots. Each of 12 port networks are defined as lumped port system in the model. Reflection coefficient of every component refers same result due to symmetric condition. With this model, electromagnetic analysis including full-wave finite element analysis is proceeded.

2.2 Radiation region boundary classification

To measure EMC characteristics of electronic motor drive systems, measurement setup and procedure should follow CISPR 25. According to the standards, the distance between receive antenna and radiator must be fixed to 1000mm in the frequency range from 150kHz to 2.5GHz. However, it is hard to analyze radiation patterns in various frequency range since radiation region boundary differs from its electrical size. Thus, our approach starts from estimating radiated electric field from frequency which has dominant radiation compared to other frequencies. Low dB of reflection coefficient refers to dominant component of transmission. Resonance point of reflection coefficient has most dominative radiative influence in overall system. For this reason, we consider the radiation pattern in resonance frequency [11].

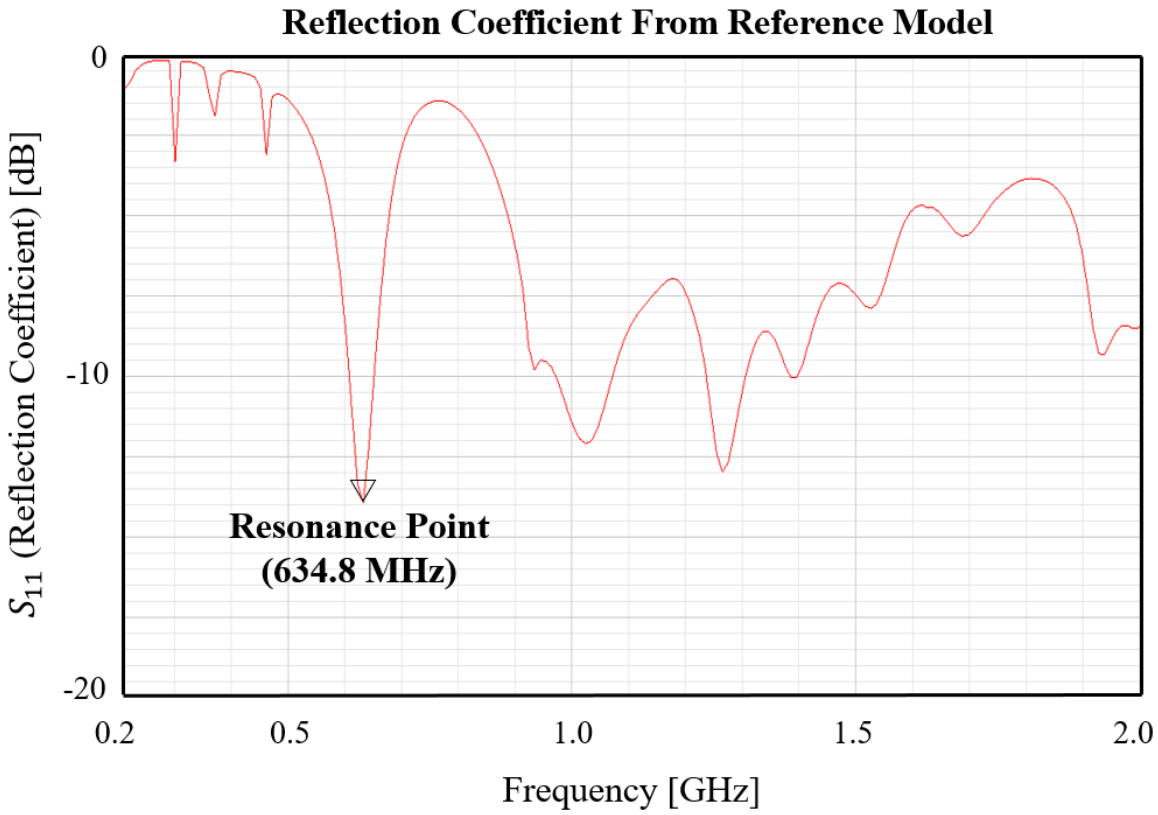

Figure 6. Reflection coefficient of reference model

Figure 6. is results of reflection coefficient of reference motor model. Resonance frequency is found by analyzing the result of 3D full-wave electromagnetic simulation. As the result, resonance frequency (634.8MHz) is pointed at the reflection coefficient plot.

Far-field condition in antenna approach also differs from its electrical size whether its electrically small or electrically large. With fixed distance, electrical size can be also vary from its frequency range. Electrical size of antenna is classified by proportion of wavelength and circumference into three region including unclear region. In condition of stator winding parameters, circumference of single winding loop can be calculated as C = 0.704m. With this value, we can classify its electrical size as various frequency range. Electrical size classification including its requency range is arranged in Table 2 [12].

Table 2. Electrical size classification

Electrical Size	Size condition	Frequency Range
Electrically small	$C < \lambda/10$	$f < 42.6MHz$
Unclear	$\lambda/10 < C < 2.5\lambda$	$42.6MHz < f < 1065MHz$
Electrically large	$2.5\lambda < C$	$1065MHz < f$

Resonance point of proposed model is in unclear region. In other words, radiation region boundary classficaition is ambiguous. To define the radiation type in unclear cases, the rates of error between the measured 1000mm radiation and far-field radiation patterns are considered. The error rate in frequency range of 100MHz to 900MHz is plotted in Figure 7. In given resonance frequency point, rms error rate refers less than 5%. As the result, radiation in target frequency can be analyzed as far-field radiation [11].

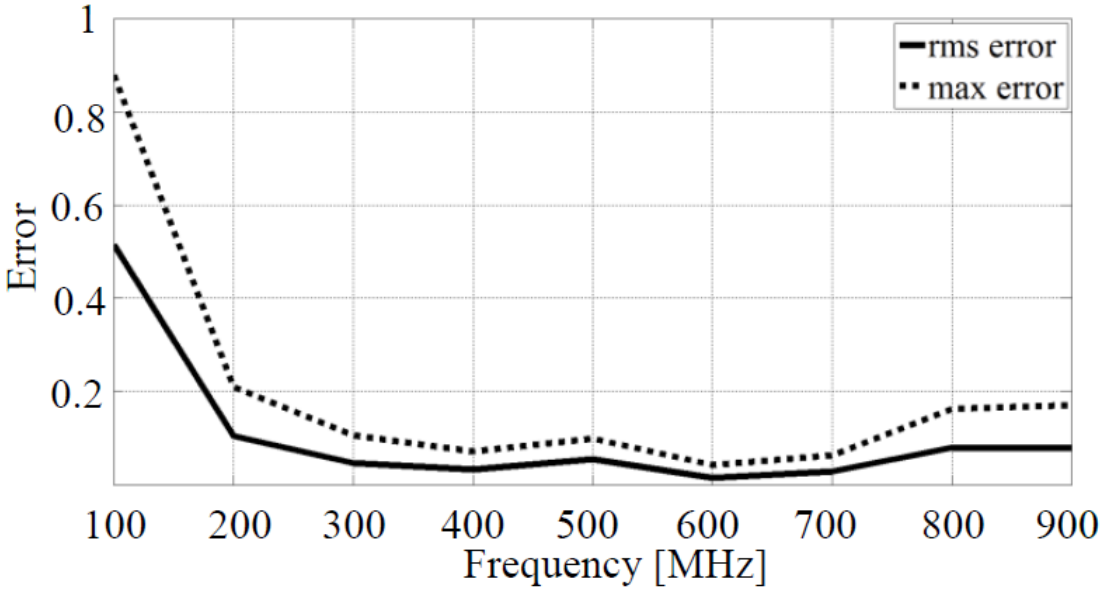

Figure 7. The error rate of the radiation patterns the far-field radiation and measured at 1m

2.3 Estimation of radiation pattern with 3D full-wave electromagnetic simulation

As mentioned in previous section, radiated electric field can be obtained using 3D model simulator. It is possible to analyze radiation pattern in perspective of every angle of theta (θ) and pi (ϕ) by using full-wave finite element method (FEM). In condition of CISPR 25 standards, measurement distance is fixed in 1m. Thus, radiation pattern which is expressed in terms of multiplication of radiation distance and radiated electric field intensity is scaled in volts.

To analyze far-field radiation pattern in three-phase motor winding under three-phase voltage excitation, we can consider harmonic frequency (f_h) that is the integer multiple of fundamental line frequency (f_o).

$$f_h = N_h \times f_o = (3M + k) \times f_o$$

For $k = 1$, the excitation of three-phase motor involves in the sequence of original phase. Stator winding operates normally in condition of winding structure. For $k = 2$, the excitation of three-phase motor involves in reverse sequence of original phase. However, stator winding operates equally with $k = 1$ due to the symmetric winding structure. For $k = 0$, the excitation of three-phase motor has equal phase.

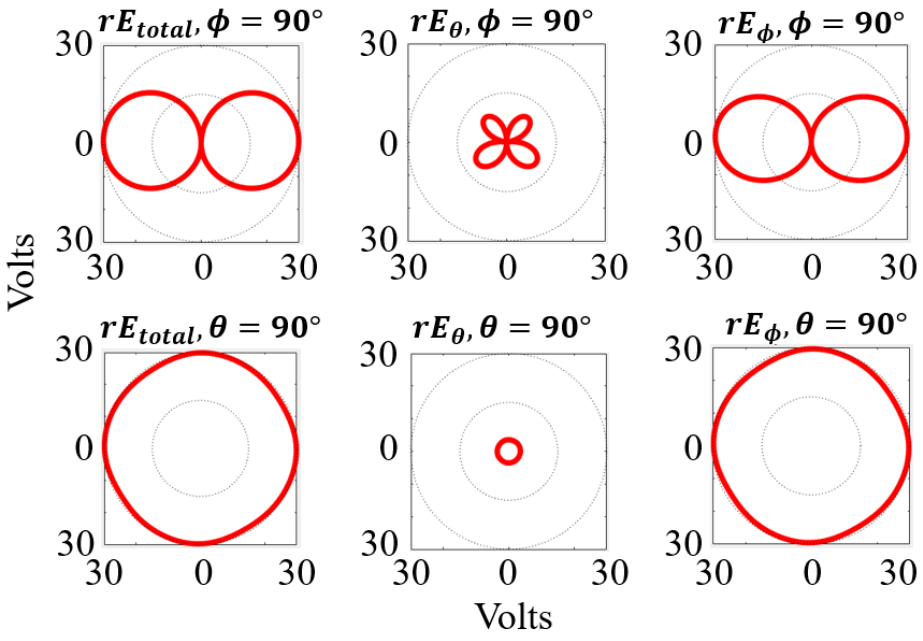

Figure 8. Radiated electric fields (in volts scale) when harmonic factor $k = 1$ or 2 at $\phi = 90°$ and $\theta = 90°$ by 3D-full wave electromagnetic simulation

Figure 8. illustrates far-field radiation patterns of the case when harmonic factor of excitation is $k = 1$, 2. For these cases, each lumped port is excited with 1W source equivalently. To compare the result from the case of $k = 1$ and $k = 2$, the result indicates same pattern due to only changes are the sequence of phase. By comparing radiation patterns from (rE_{ϕ}) and (rE_{θ}), ϕ directional which is end-winding component of stator winding have dominant radiation.

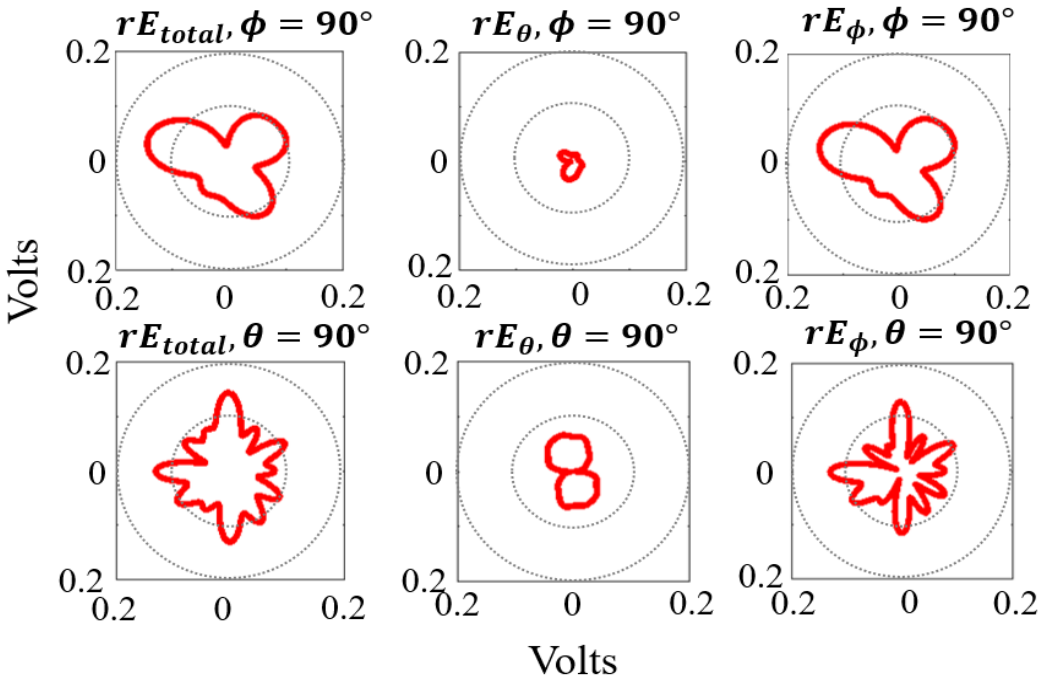

Figure 9. Radiated electric fields (in volts scale) when harmonic factor $k = 0$ at $\phi = 90°$ and $\theta = 90°$ by 3D-full wave electromagnetic simulation

Figure 9. illustrates far-field radiation patterns of the case when harmonic factor of excitation is $k = 0$. Ideally, radiation pattern should be in non-value result due to its balanced current distribution of three-phase coils. FEM simulation results illustrates radiation pattern scale of 0.2. However, the result indicates almost zero volts for every component compared to the case when $k = 1$ or 2.

Chapter III

Array antenna approach to analyze radiation in ac motor

The radiation region boundary classification including far-field condition is proceeded in the previous discussion. EMC analysis through the proposed model in resonance frequency (634.8MHz) can be concerned in the far-field radiation. Thus, the radiation pattern from stator winding of ac motor can be analyzed regardless of distance between radiator and receiver [11].

3.1 Theoretical approach to estimate radiation pattern

Array antenna model to approach the radiation pattern from the stator winding starts with assumption of each coil loop as single radiator antenna. Moreover, structure of winding array forms circular array of antenna radiator. Since slot winding in stator forms tetragonal shape, each loop winding consists 4-directional current distribution which are two axial components and two end-winding components. The single loop excitation component is illustrated in Figure 10.

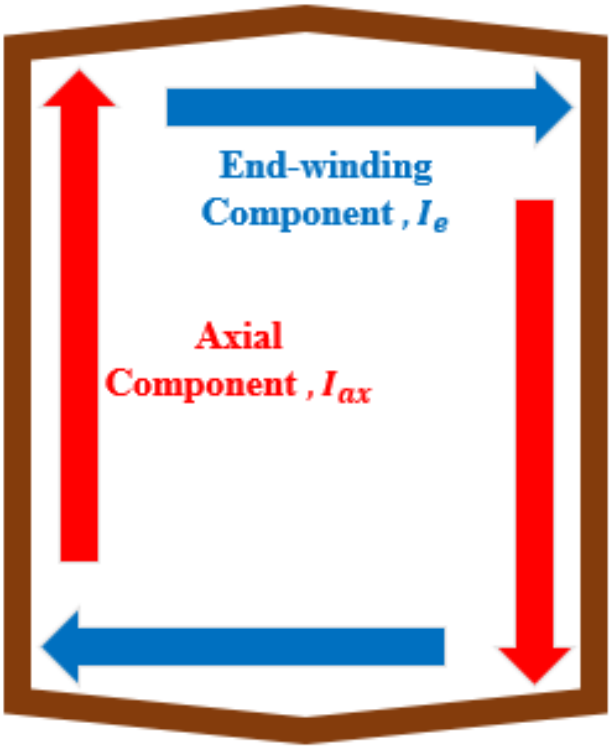

Figure 10. Current distribution of single loop winding

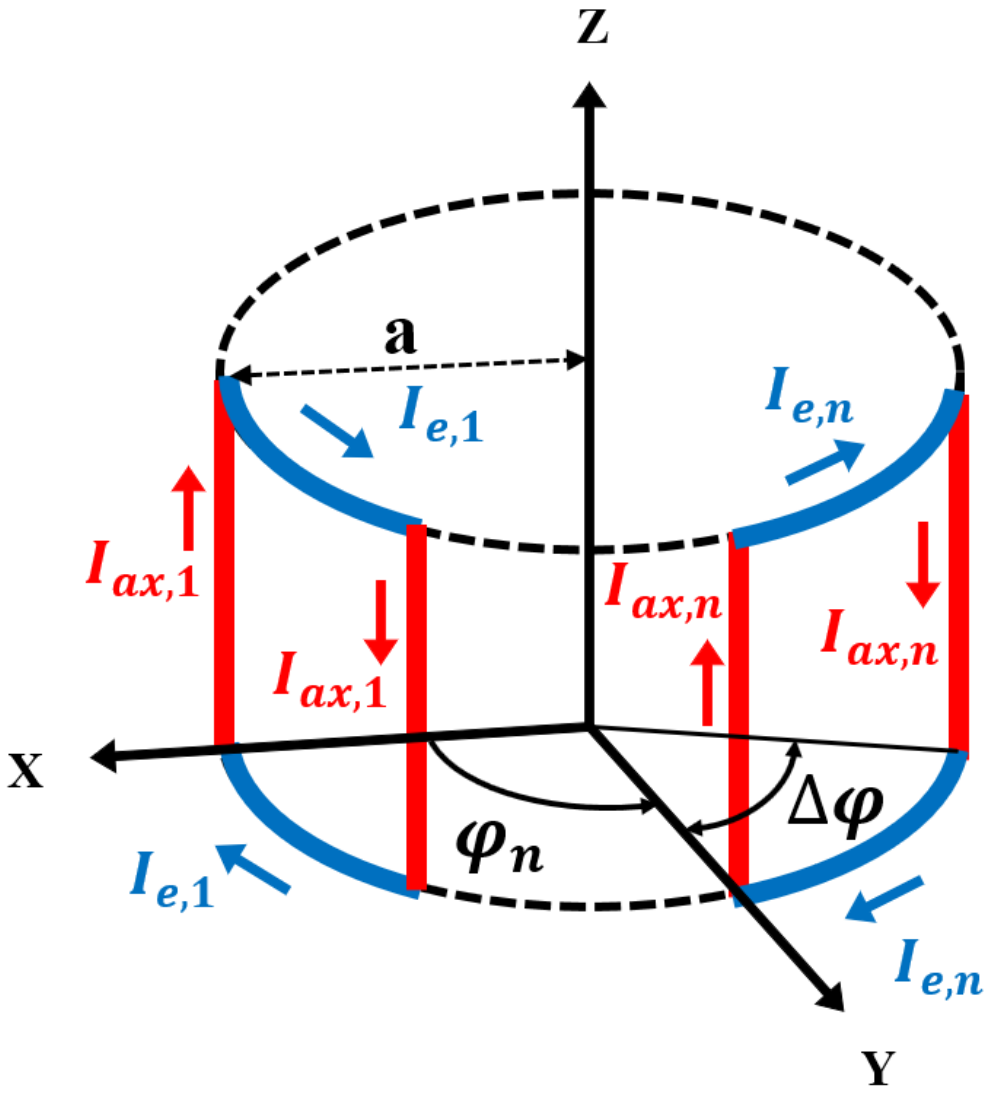

Figure 11. Simplified stator winding model distributed in 3D coordinate plane

Since stator winding coil has two different vector component, overall magnetic vector potential can be independently calculated by sum of its axial component and end-turn component [12]. Overall magnetic vector potential can be expressed as follows:

$$\boldsymbol{A} = A_{\varphi}\hat{\boldsymbol{\varphi}} + A_z\hat{\boldsymbol{z}}$$

To calculate magnetic vector potential of proposed method, derivation of current source distribution is initial process. When the loop length of the coil is the free-space wavelength at the resonance frequency, the spatial current distribution component has sinusoidal and co-sinusoidal excitation. By the right-angle condition of azimuthal direction and axial direction, independent current distribution of axial array can be expressed as follows:

$$I_{ax,n} = I_n e^{ja_n} i_{ax}(z)\delta(\rho - a)\delta(\varphi - \varphi_n)\hat{\boldsymbol{z}}$$

$I_n e^{ja_n}$ is the phase current excited to the n-th element. i_{ax} is the current distribution of axial component. φ_n is the azimuthal angle location of n-th element. Magnetic vector potential equation can be obtained from integral of overall axial current distribution which is expressed as follows:

$$A_z = \left[\frac{\mu e^{-j\beta r}}{4\pi r} a \int_{-\frac{l_{ax}}{2}}^{\frac{l_{ax}}{2}} i_{ax}(z') e^{j\beta a z' \cos\theta} dz'\right] \times \sum_{n=1}^{N} I_n e^{j\alpha_n} e^{j\beta a \sin\theta \cos(\varphi - \varphi_n)}$$

Derivation of end-winding current source component is similarly proceeded within axial component. Unlike axial component, end-winding component should be divided into two parts since opposite direction of top and bottom side should be concerned. Thus, the classified current distribution can be expressed as follows:

$$I_{e,n}^{\pm} = I_n e^{j\alpha_n} i_e\left(a\left(\varphi - \varphi_{n+\frac{\Delta}{2}}\right)\right)\delta(\rho - a)\delta\left(z \mp \frac{l_{ax}}{2}\right)\hat{\boldsymbol{\varphi}}$$

Likewise, magnetic vector potential equation of end-winding component can be expressed in sum of end-winding current distribution as follows:

$$A_\varphi = \frac{\mu e^{-j\beta r}}{4\pi r} a \cos\left(\beta \frac{l_{ax}}{2} \cos\theta\right) \times \sum_{n=1}^{N} \left[\int_{-\frac{\Delta\varphi}{2}}^{+\frac{\Delta\varphi}{2}} i_e(\xi) e^{j\beta a \sin\theta \cos\left(\varphi - \xi - \varphi_{n+\frac{\Delta n}{2}}\right)} d\xi\right] I_n e^{j\alpha_n}$$

Thus, two independent vector components can be obtained. With the calculated magnetic vector potential value, electric field equation (**E**) can be derived in terms of magnetic vector potential as follows:

$$\mathbf{E} = -j\omega\mathbf{A} - \frac{\nabla(\nabla \cdot A)}{\omega\mu\varepsilon}$$

Radiated emission of three-phase motor in condition of CISPR 25 are in region of near-field radiation. However, the far-field radiation pattern can be obtained due to relatively small error between the near-field radiation and far-field radiation. Second term of derived electric field equation can be neglected. Thus, derived electric field equation can represent magnetic vector field in independent component of theta direction ($\boldsymbol{\theta}$) and pi direction ($\boldsymbol{\varphi}$). The simplified electric field equation can be expressed as follows:

$$\mathbf{E} \approx -j\omega\mathbf{A} = j\omega \sin\theta\, A_z \hat{\boldsymbol{\theta}} - j\omega A_\varphi \hat{\boldsymbol{\varphi}}$$

3.2 Mutual coupling effect among excitation of looped winding

To analyze radiation pattern from stator winding structure model, mutual coupling effect among coil loop cannot be neglected since coils are closely wound. Radiation patterns calculated by array antenna theory do not concerns mutual coupling effect. Due to unbalanced coupling, ideal current source has unappropriated magnitude and phase. Compensation process is required to calculate more realistic array antenna calculation results [13].

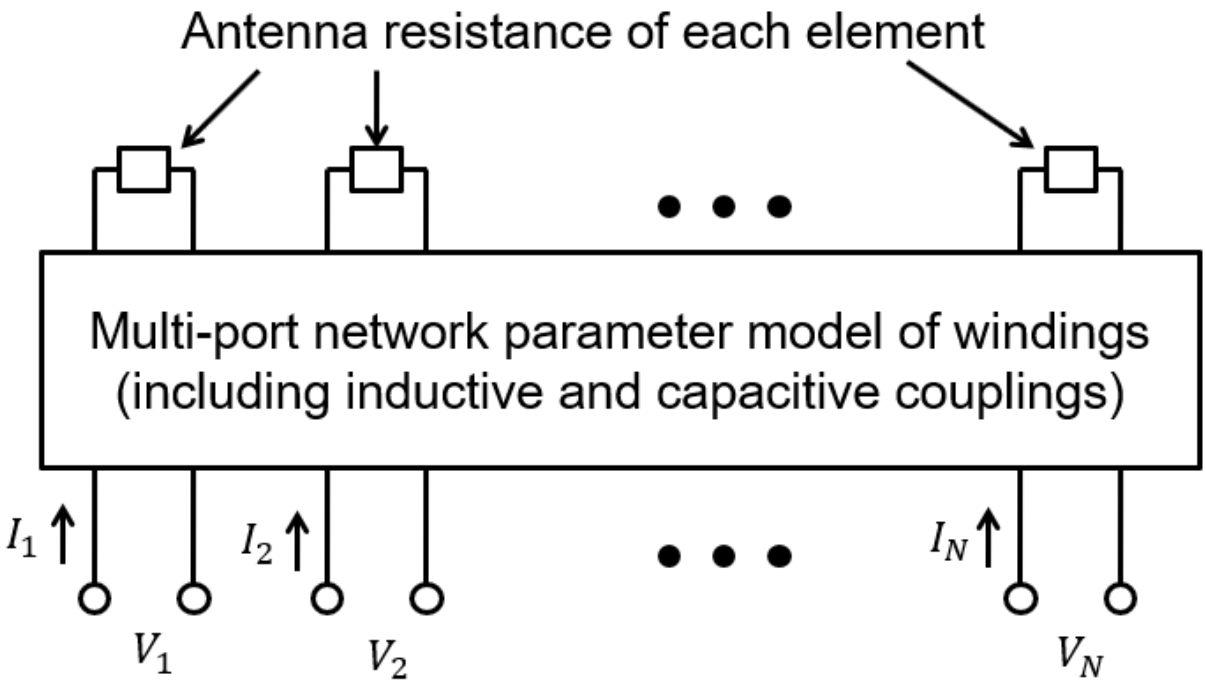

Figure 12. Mutual coupling compensation network

Multi-port RLC network circuit model can be suggested to compensate degrade of coupling effect. The proposed circuit model can be constructed by integral equation based RLC extraction tool. By applying the circuit model, modified current source element is alternatively involved to calculate appropriate radiation pattern.

Figure 12. indicates multi-port network parameter model of windings including inductive and capacitive couplings. With calculated impedance value for every port network, compensated current source for each port is rearranged.

Before compensation of mutual coupling effect, where antenna impedance of 42.1757Ω and port excitation of 1W, magnitude of current source for each port antenna radiator is calculated as follows:

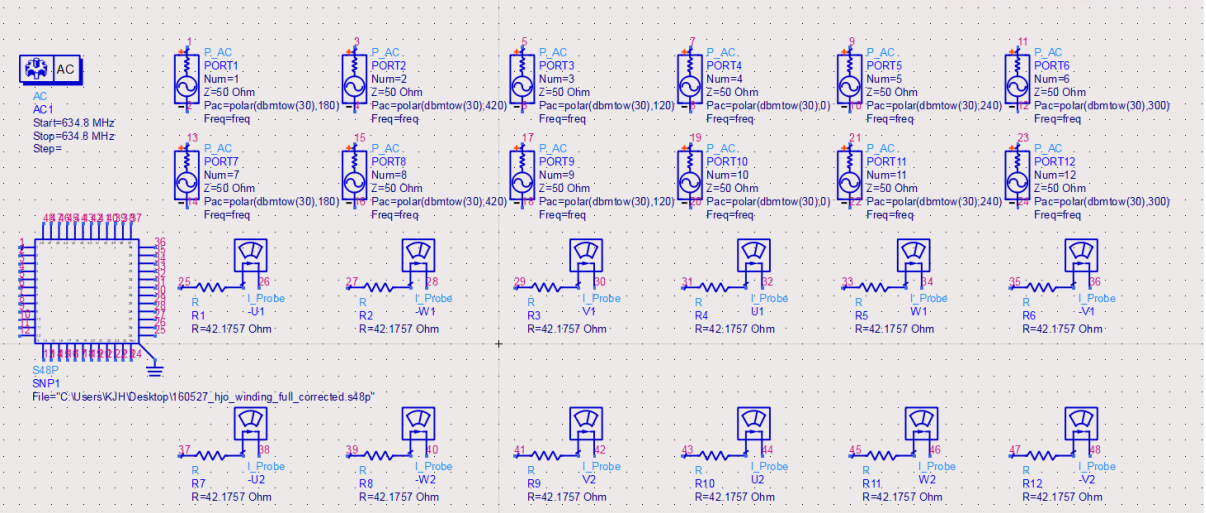

Figure 13. 48-port network simulation to calculate magnitude and phase of source current

By applying RLC extract tool, compensated amplitude and phase for each phase is obtained. Amplitude of each phase have different amplitude. This value might degrade symmetric condition of expected value but compensate mutual coupling effect.

3.3 Analysis of radiation pattern between simulation results and array antenna method

In condition of CISPR 25 standards, 1m distance is fixed in target frequency range. The radiation pattern field can be scaled in volts in terms of multiplication of measured electric field and the distance of between radiator and receiver. Thus, the radiation pattern measured from simulation model and calculated far-field radiation pattern should result in identical.

The magnitude of radiated electric field from three-phase motor stator winding is calculated within assumption of stator winding coil as circular array of antenna. The calculated electric field can be represented in two directions of theta direction and pi direction.

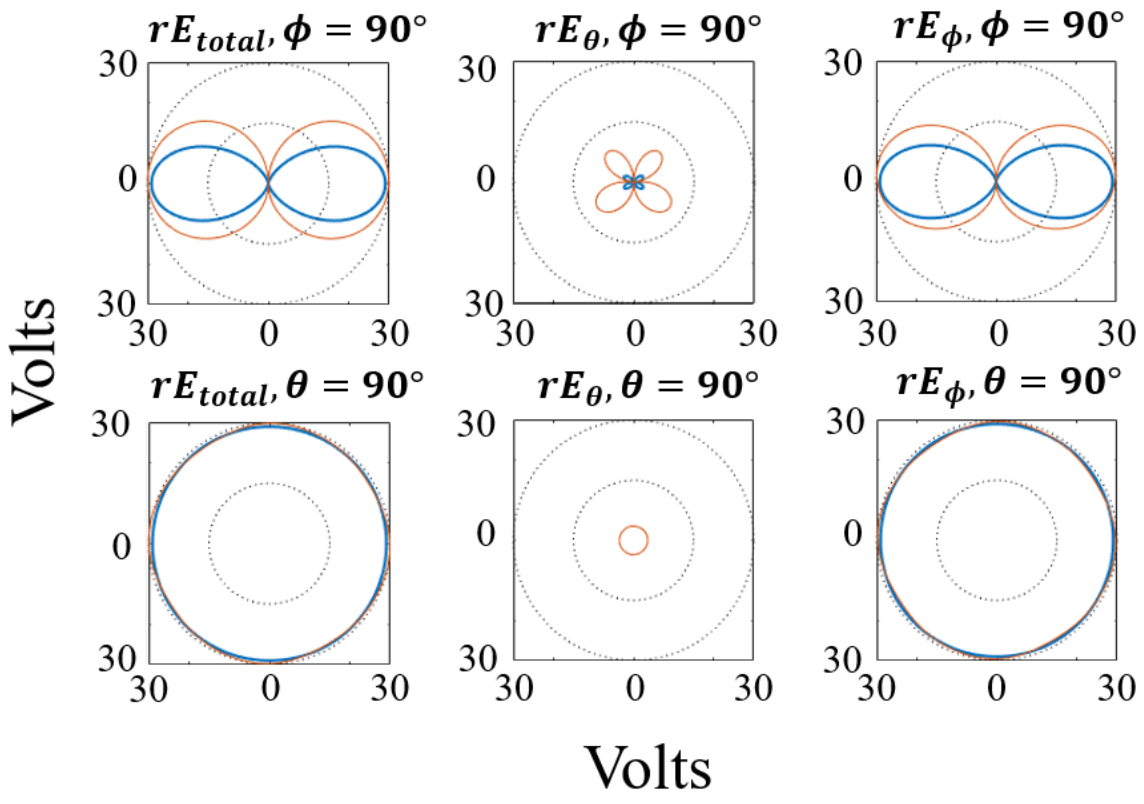

Figure 14. Radiated electric fields (in volts scale) when the harmonic factor k = 1 or 2. $\phi = 90°$ and $\theta = 90°$ (Blue: 3D full-wave finite element method, Orange: array antenna calculation)

Figure 14. represents comparison of far-field radiation patterns from simulation model and calculated results in cases of k = 1 or 2. Two cases have same value for both simulation results and calculation results. For both cases, current source is excited in 1W. Upper three patterns indicate radiation pattern at $\phi = 90°$. Lower three patterns indicate radiation pattern at $\theta = 90°$. Both radiation patterns show that ϕ-directional component have dominant radiation compared to θ-directional component. These two results show relatively similar results with resemble in shape. In radiation pattern at θ-direction at $\theta = 90°$, simulation result has existed value, but array antenna calculation results in empty pattern.

For harmonic factor k = 0 case, radiation pattern from array antenna calculation doesn't show anything. Ideally, the magnitude of far-field radiation is 0 due to the suppression of overall current distribution from each other. Simulation result from 3D model FEM shows non-zero value for all cases. However, it has relatively low value level of radiation compared to case of harmonic factor k = 1 or 2 cases.

3.4 Additional winding model analysis

To double check performance of array antenna method in stator winding, additional winding model is proposed. This model has single-layer fractional slot winding structure which is also known as tooth-coil structure. The fractional slot windings with extremely small fractions are popular in brushless DC machines and permanent magnet synchronous machines (PMSMs).

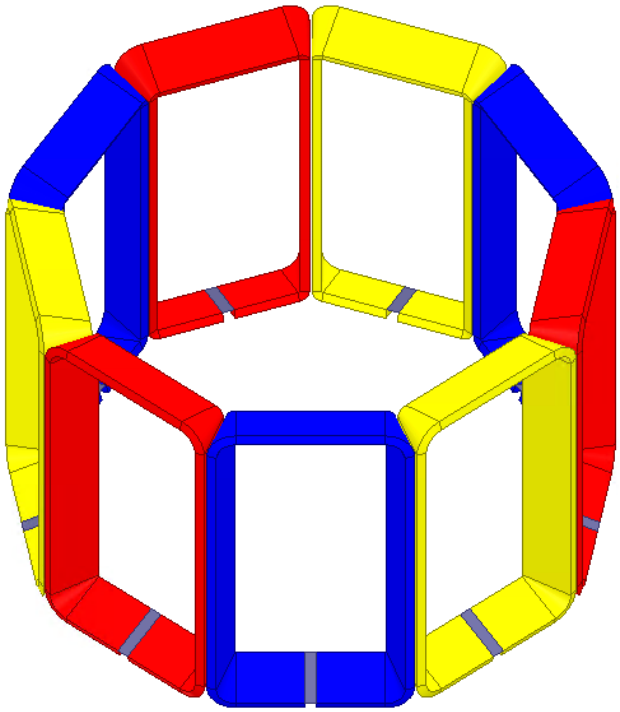

Figure 15. Stator winding structure of additional model

This structure contains two different phase coils in a every single slot. Simulation model is figured in Figure 15. and specific winding parameters are shown in Table 3. Axial length of coil, turn numbers and diameter of the stator followed same value with previous model. However, slot number, Q has reduced to 9 even though number of pole pairs, p has increased to 3 in identical three-phase ac motor operation. The number of slots per pole and phase, q can be calculated as follows:

$$q = \frac{Q}{2pm} = \frac{9}{2 \times 3 \times 3} = \frac{1}{2}$$

Table 3. Motor parameters of tooth-coil model

Parameters	Value
Slot number, Q	9
Pole number (Pole pairs, p)	6(3)
Phase, m	3
Number of slots per pole and phase, q	1/2
Pole pitch	1
Turn number	12
Port excitation [W]	1.333
Axial coil length [mm]	210
Stator diameter [mm]	290

Resonance frequency can be changed due to difference of winding structure. Therefore, finding resonance frequency for newly designed model is essential procedure. By the same method with previous model, resonance point can be found by plotting the reflection coefficient of lumped port excitation. As the result, resonance frequency (925.1MHz) for this model is pointed at Figure 16.

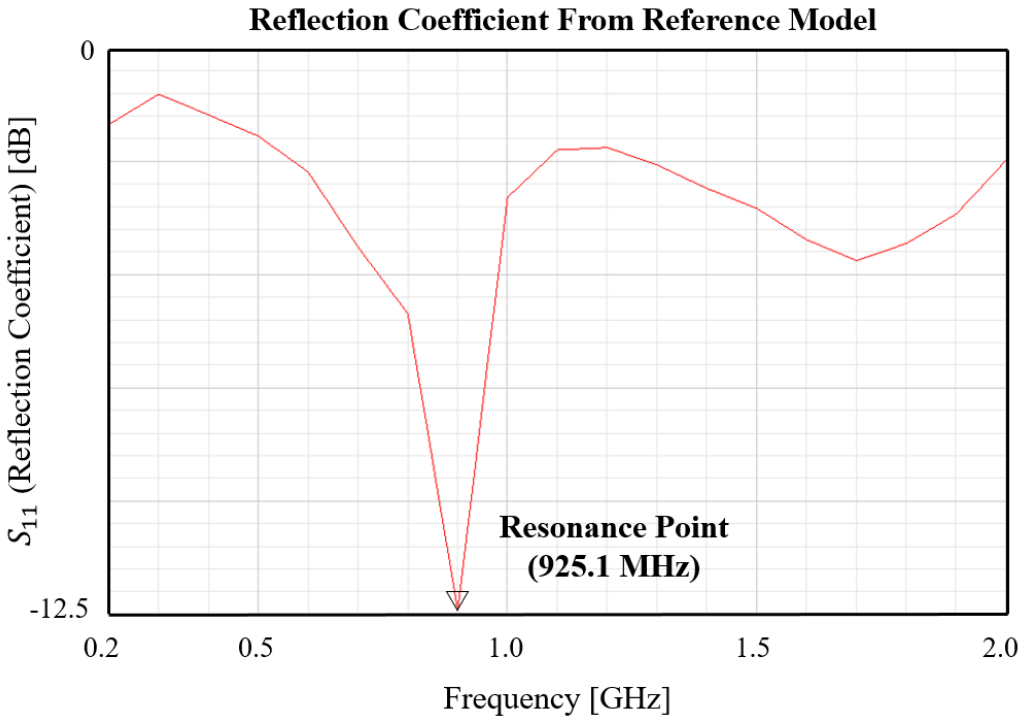

Figure 16. Reflection coefficient of additional model

To compare radiation patterns with previous model, not only shape of the patterns but also magnitude of radiated emission is important factor to consider. Magnitude of radiation pattern is directly related with current source excitation. Thus, current source must have identical port excitation level with previous model. This model involves 1.333W excitation for overall 9 coils which has same level of 12 coils excited with 1W for previous model.

Radiation region boundary condition of tooth-coil model remains same since there is no change in mechanical parameters. Similarly, radiation from new model can be analyzed in far-field radiation region. Comparing 3D-full wave FEM simulation in case of harmonic factor k = 1 or 2 is initial process to justify suitabiltiy of new model.

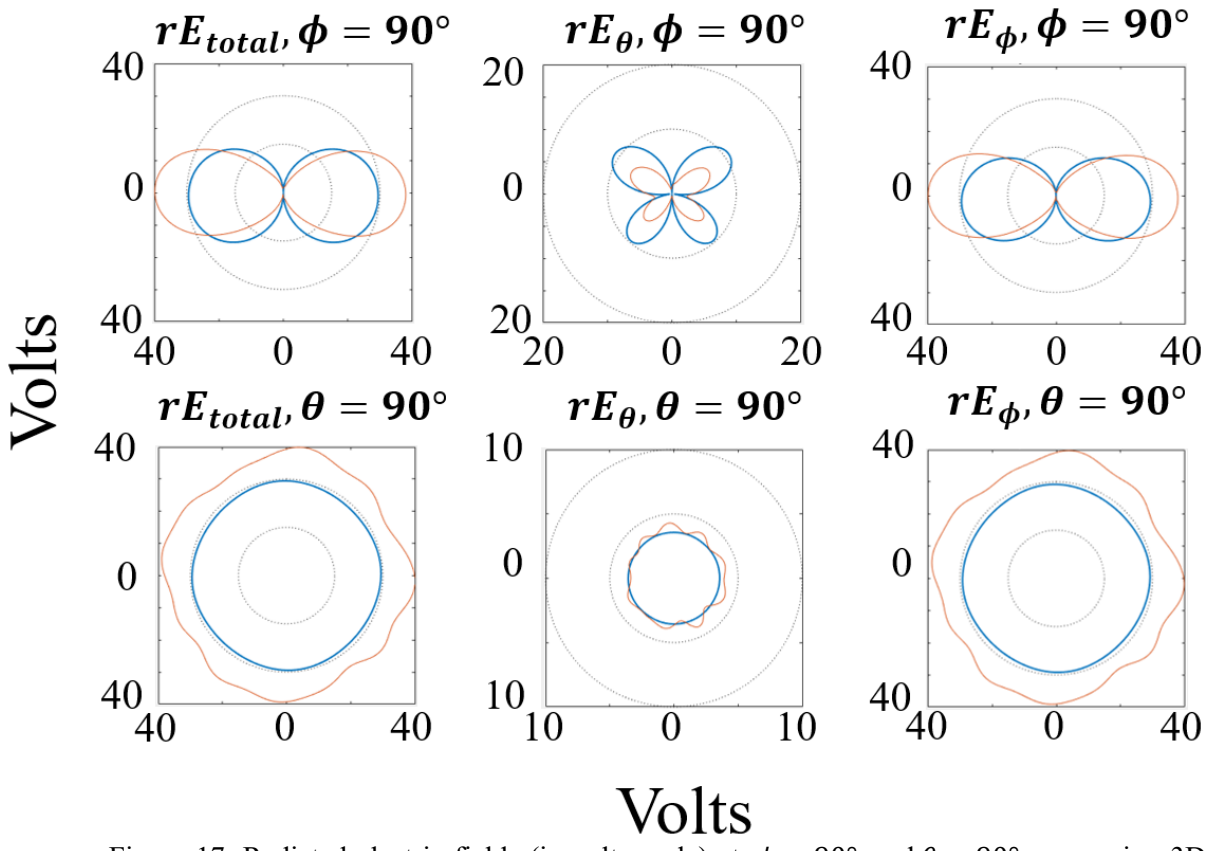

Figure 17. Radiated electric fields (in volts scale) at $\phi = 90°$ and $\theta = 90°$ comparing 3D full-wave finite element method simulation results (Blue: Integral slot winding model, Orange: Tooth-coil model)

Figure 17. indicates comparision of radiation pattern obtained from 3D full-wave FEM simulation between integral slot winding model and tooth-coil model. According to figure, new proposed model represent stronger magnitude of radiation in overall cases. Radiation pattern when $\theta = 90°$ shows

more unstable results compared to original model. However, both simulation results found dominative radiated emission source from end-winding component compared to axial component.

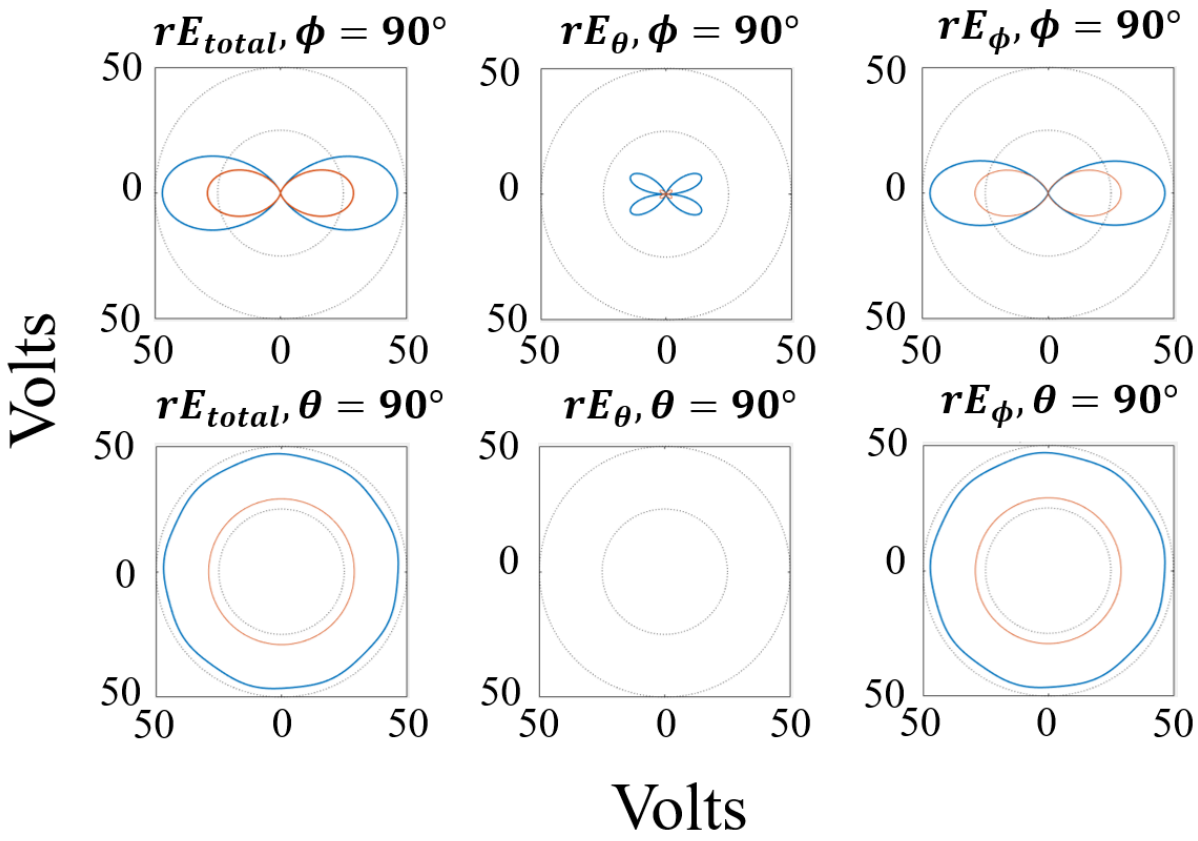

Figure 18. Radiated electric fields (in volts scale) at $\phi = 90°$ and $\theta = 90°$ comparing array antenna calculation results (Blue: Tooth-coil model, Orange: Integral slot winding model)

Figure 18. shows radiation patterns calculated by array antenna method. Tooth-coil model has even greater magnitude of radiation compared to simluation results. This can result in fractional slot-winding has more radiative component compared to integral slot-winding. Likewise, axial component when $\theta = 90°$ indicates zero value since theoritical current distribution suppress each other. Calculation results also indicates that end-winding component has dominative radiation in three-phase motor winding. Compared to simulation results, calculation results shows more exquisite relation but more difference in magnitude of radiation

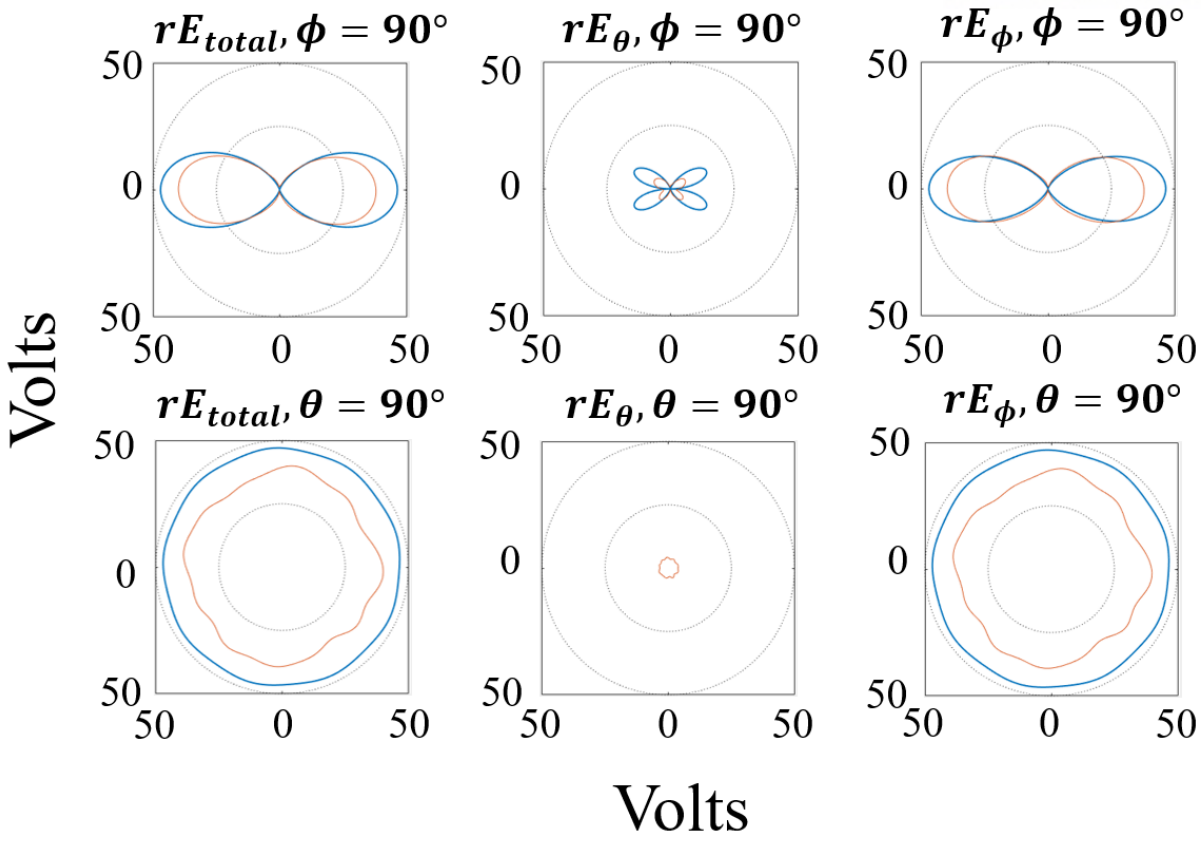

Figure 19. Radiated electric fields (in volts scale) at $\phi = 90°$ and $\theta = 90°$ comparing simulation results and array antenna calculation of tooth-coil model (Blue: Array antenna calculation, Orange: 3D full-wave finite element method of tooth-coil model)

Figure 19. refers comparison of radiation patterns from 3D full-wave FEM simulation and array antenna calculation when harmonic factor k = 1 or 2. Compare to integral slot winding model, port excitation level has been matched by controlling input current source. Nevertheless, magnitude of overall radiation shows greater value due to adjacent condition of winding coil. In the case when $\phi = 90°$, radiation patterns show same directional pattern with similar magnitude. When $\theta = 90°$, radiation patterns indicate similar shape and magnitude. In general, integral slot winding model refers more accurate results. However, tooth-coil model also represents similar result in every radiation pattern. Thus, array antenna approach is considerable method for measuring radiation patterns from stator winding of AC motor drive.

Chapter IV

Measurement setup

To measure radiation in antenna chamber, realistic synchronous motor cannot be measured directly due to its weight. However, plastic fixture only containing winding structure neglecting magnetic core and rotor model can be substituted. Enamel copper wire, frequently used in electric motor, is wound in sequence of winding method proposed in previous chapter. The combined structure can take role as three-phase motor. The overall layout is figured in Figure 20.

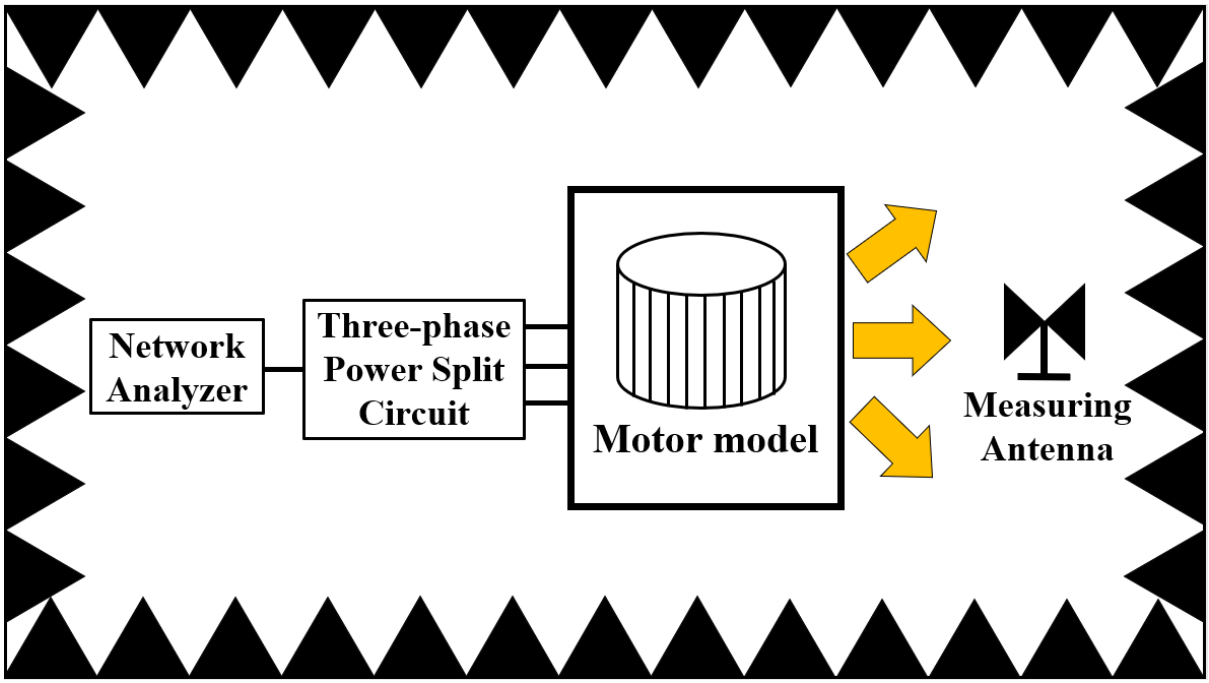

Figure 20. Diagram of overall layout of measuring radiation pattern in antenna chamber

Two kinds of three-phase power circuit are also designed for measurement. Each case is designed to classify input sources according to its harmonic factor (one for $k = 0$, the other for $k = 1$ or 2). Both circuits are consisting 4 ports of SMA connector connected through RF power splitter and microstrip transmission line. For $k = 0$ case, length of transmission line from splitter to every port are the same. However, for $k = 1$ or 2 case, length of transmission line is regulated by phase shifting method and derivation is shown below.

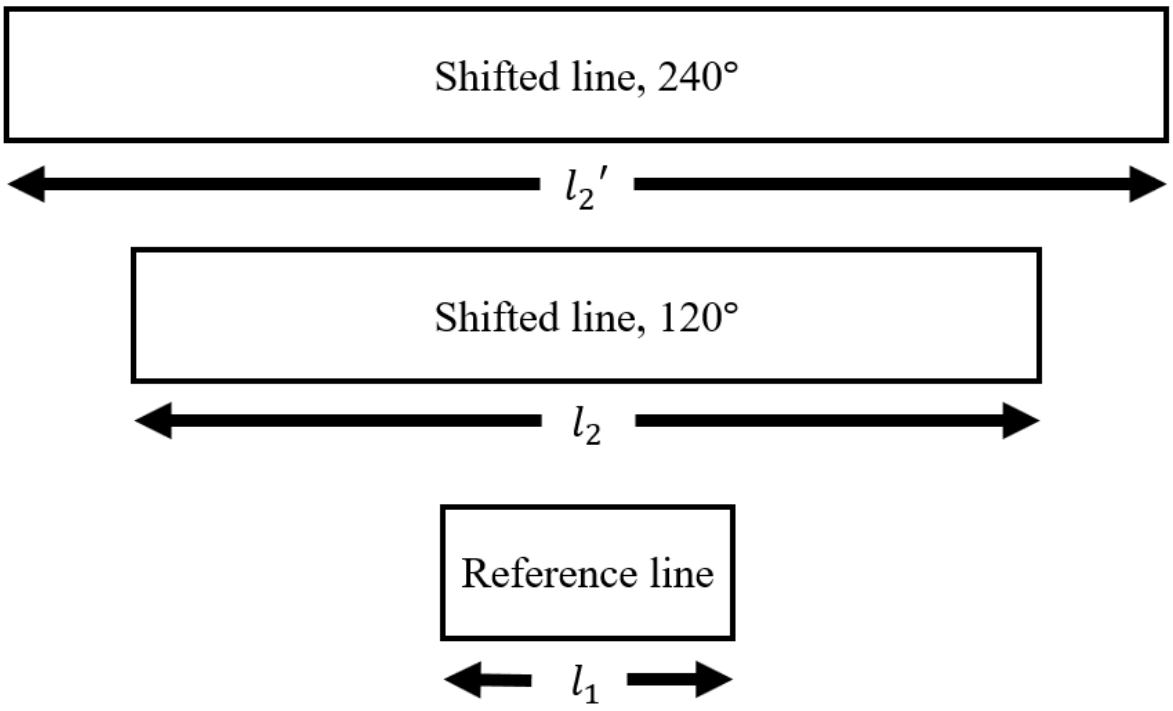

Figure 21. Design of three-phase power split circuit

To design three-phase power split circuit, designed circuit must be splitting equivalent power level into each difference phases tuning 120 degrees while retaining matched impedance. Basic theory follows from regulating electrical length of microstrip transmission line in dielectric PCB [14].

In order to design the phase difference of 120° shifted line, the equation of transmission line is derived below:

$$\Delta\emptyset = \beta(l_2 - l_1) = \beta\Delta l$$

Firstly, target phase difference in radian should be fixed to obtain electrical line difference. Where $\Delta\emptyset$ stands for target phase difference, Δl stands for target length difference of microstrip transmission line.

$$\Delta\emptyset = 120^{\circ} = \frac{120}{360} \times 2\pi = 2.094\, rad$$

$$\lambda_{air} = \frac{c}{f} = \frac{3 \times 10^8}{634.8 \times 10^6} = 0.473m$$

(Where, ε_{eff} = effective dielectric constant, λ = wavelength)

$$\lambda_g = \frac{\lambda_{air}}{\sqrt{\varepsilon_{eff}}} = \frac{0.473}{\sqrt{4.7}} = 0.218m$$

$$\beta = \frac{2\pi}{\lambda_g} = \frac{2\pi}{0.225} = 28.823$$

$$\Delta l = \frac{\Delta \emptyset}{\beta} = \frac{2.094}{27.864} = 0.0727m = 72.7mm$$

For the case of third phase line, 240° shifted line, doubled length (145.4mm) is applied.

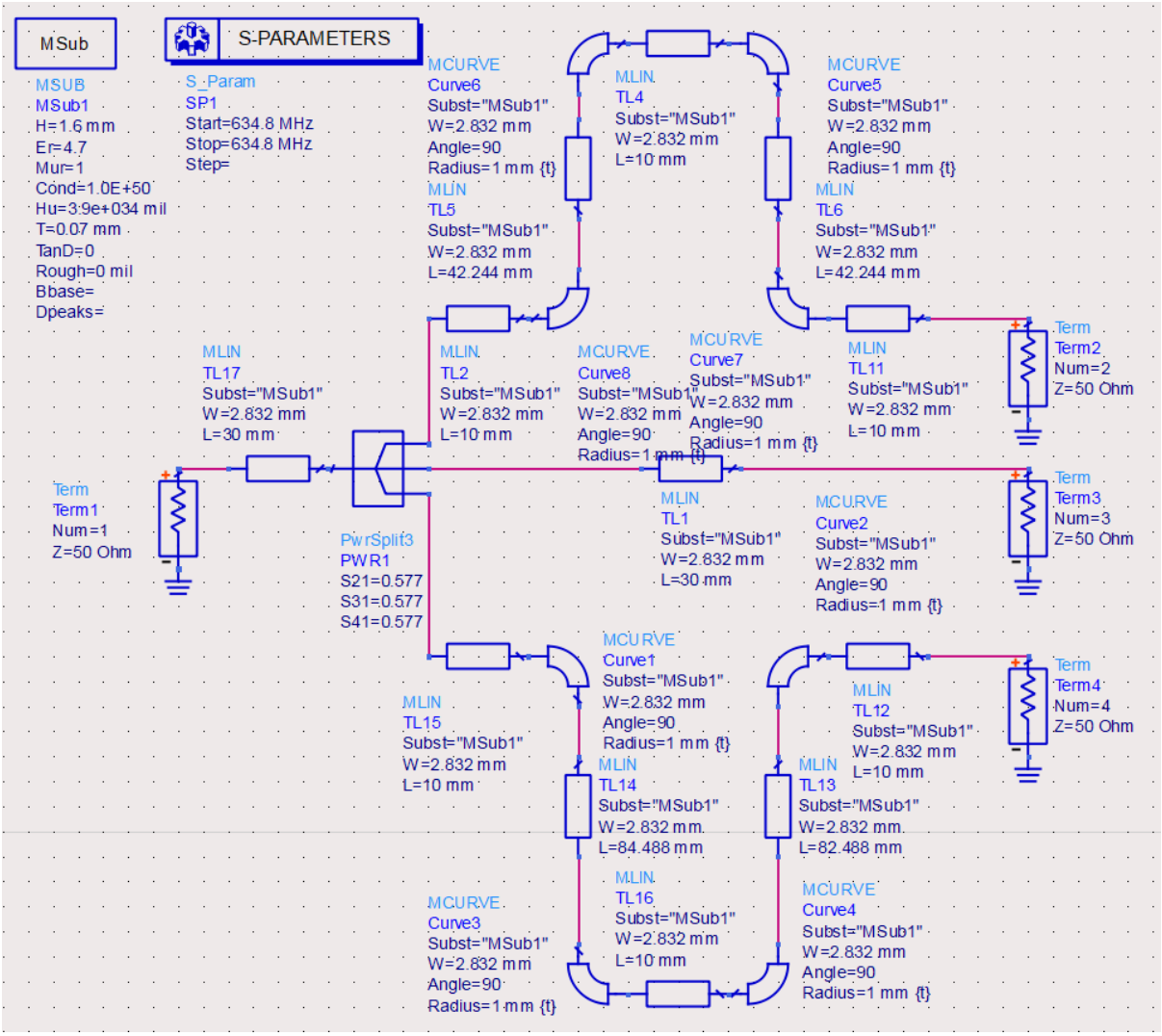

Figure 22. Layout of three-phase power split circuit designed in ADS simulator

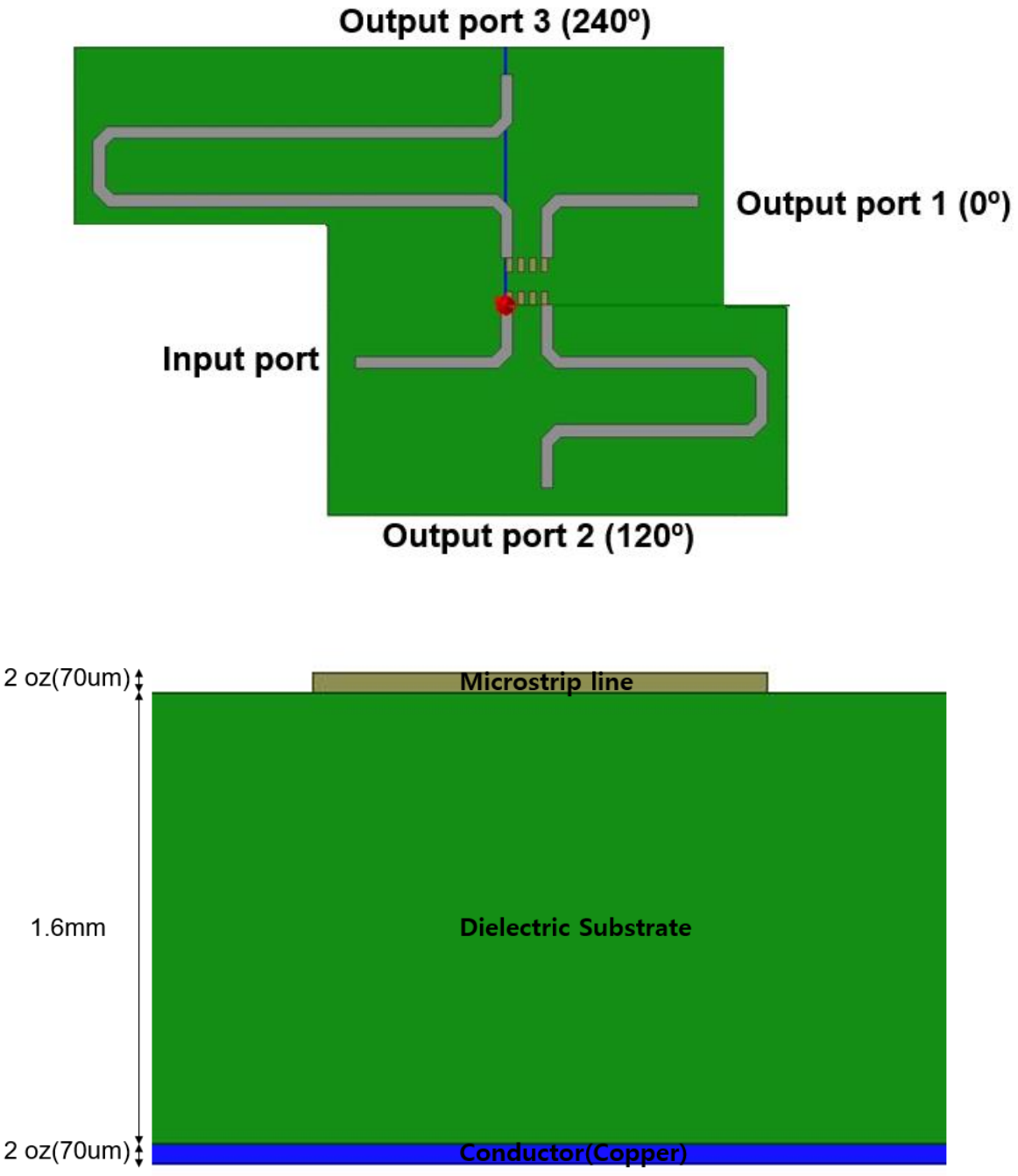

Figure 23. Layout of three-phase circuit HFSS simulation model (top view, side view)

Before designing layout, simulation using Q3D simulation must be proceeded to double-check the result of phase shifting. Figure 23. illustrates layout of the top view(X) and side view(Y) of circuit designed in HFSS.

Figure 24. is picture of PCB when the harmonic factor $k = 0$. Three-way power splitter is positioned in center. Length of all three microstrip lines are same. It is designed to have all three phases in the case when each port excitation suppresses each other.

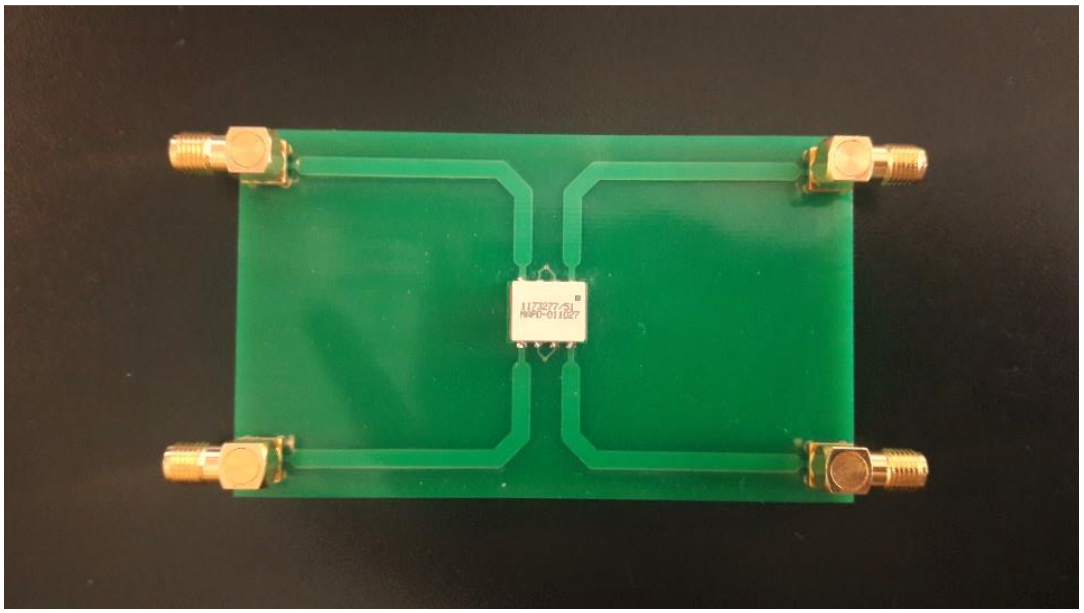

Figure 24. PCB of three-phase power split circuit ($k = 0$)

Figure 25. is picture of PCB when the harmonic factor $k = 1,2$. Three-way power splitter is positioned in center. Length of microstrip lines are defined in previous discuss. It is designed to have periodical sequence of original three-phases to measure radiation.

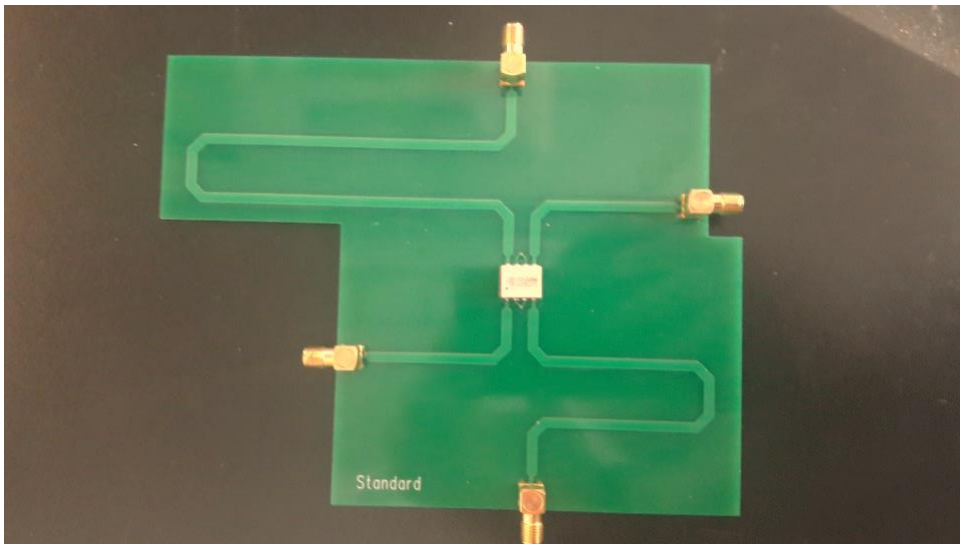

Figure 25.PCB of three-phase power split circuit ($k = 1, 2$)

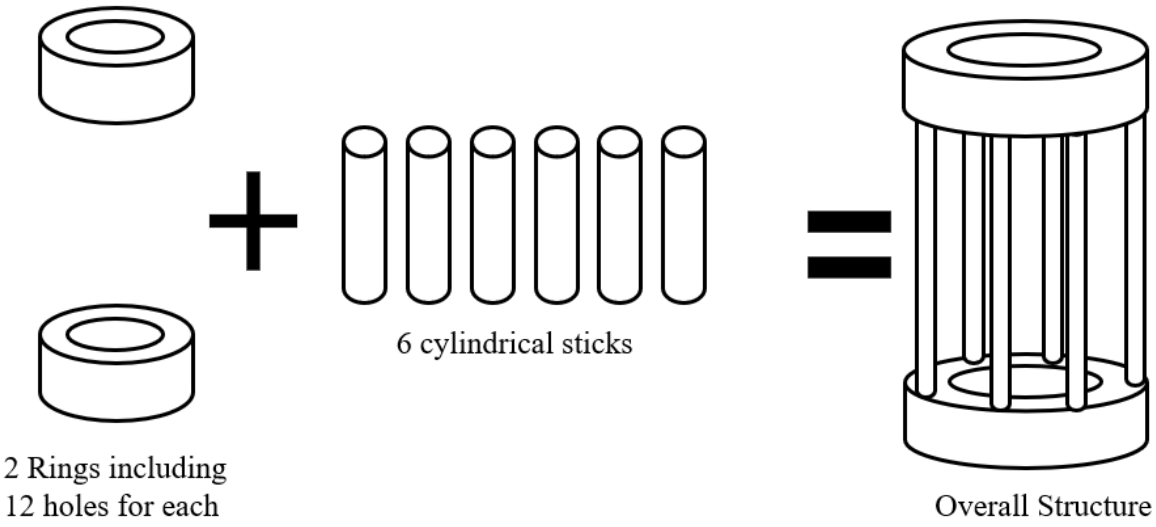

Figure 26. Structure of non-magnetic stator

Due to heavy weight of electric motor, a plastic fixture is constructed to tighten looped winding. Figure 26. indicates each belonging of structure. Substitute core is consisting 2 stator rings including 24 slot sized holes and 6 sustaining cylindrical sticks. Instead of stator core, proposed structure should sustain overall state. Designed parameters are labeled in Table 4.

Table 4. Design parameters of non-magnetic stator

Parameters	Value
Number of stator rings	2
Stator height [mm]	40
Stator outer diameter [mm]	280
Stator inner diameter [mm]	190
Number of slot holes per stator ring	24
Number of sticks	6
Stick height [mm]	130
Stick diameter [mm]	20
Material	Plastic

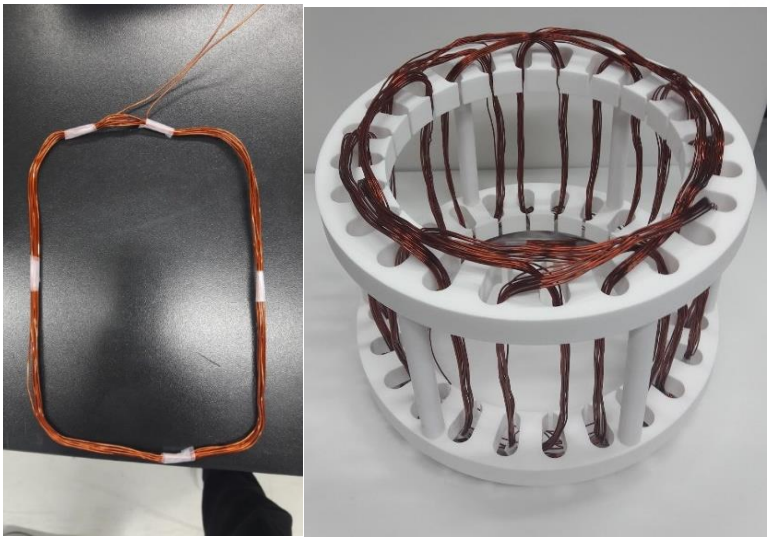

Figure 27. Single loop winding and combined structure

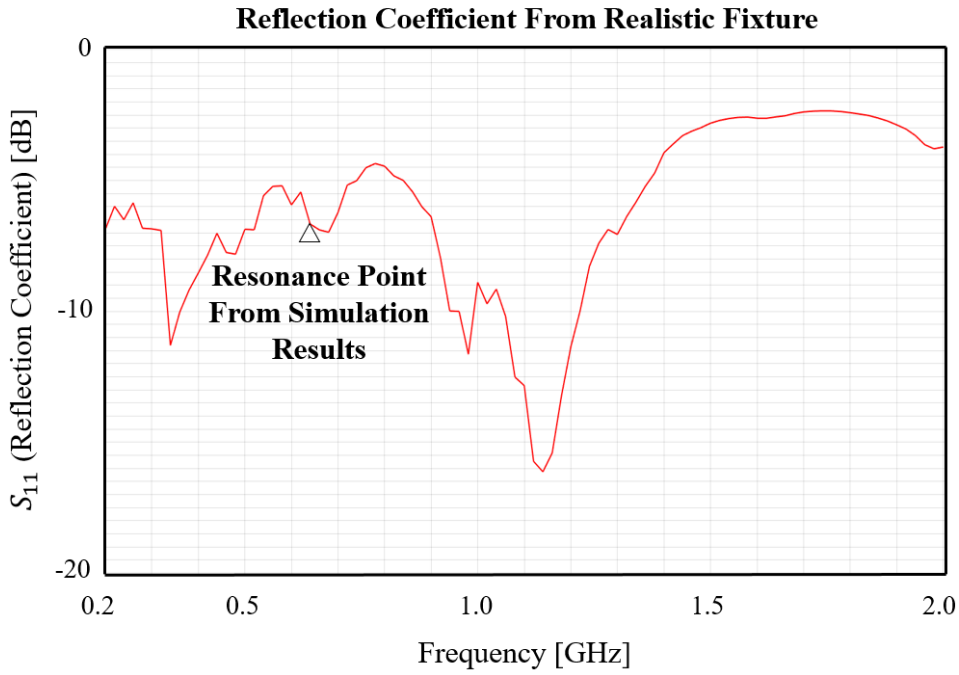

Figure 28. Reflection coefficient of realistic winding model

Before measuring electric field from realistic winding model, simulation results and realistic model must have coincided resonance point. Reflection coefficient of realistic winding model is plotted in Figure 28. However, resonance frequency gets too much different value compared to the simulation results.

CHAPTER V

CONCLUSION

In this research, array antenna method is proposed to estimate the radiation patterns from the AC motor under the CISPR 25 standards. Two different stator winding model operating in three-phase is designed to analyze radiation patterns. The 6 different radiation patterns can be plotted in polar coordinates of magnitudes in every degree. Results of radiation patterns between array antenna calculation method and finite element method made mostly coincided figure. Since the radiation region boundary varies as various frequency band, far-field condition in unclear region is defined to analyze radiation patterns. Three-phase excitation in motor operating system is related to harmonic factor in fundamental line frequency. When $k = 1$ or 2, three-phase current excitation follows sequence of stator winding. When $k = 0$, obtained radiation patterns can be hardly due to the symmetric excitation of three-phase current sources. Estimation of radiation patterns using array antenna method is done by assumption of winding structure as circular array of antenna. Multi-port RLC network model is proposed to capture the mutual coupling effect among coils. Modified current source is suggested to calculate appropriate result of array antenna approach. Stator winding structure and three-phase power split circuit is designed for measurement setup. However, different radiation patterns are obtained from measurement in antenna chamber. Debugging process of motor model design including accurate resonance point value is required for future work.

References

[1] B. Mirafzal, G. L. Skibinski, R. M. Tallam, D. W. Schlegel and R. A. Lukaszewski, "A failure mode for PWM inverter-fed AC motors due to the antiresonance phenomenon," *IEEE Trans. Industry Applications*, vol. 45, no. 5, pp. 1697-1705, Sep./Oct. 2009.

[2] Firuz Zare, "EMI in Modern AC Motor Drive Systems," *IEEE EMC Society Newsletters,* summer 2009; pp.53-58.

[3] Degano, M., Zanchetta, P., Clare, J. Empringham, "HF induction motor modeling using genetic algorithms and experimental impedance measurement," *Industrial Electronics, 2010 IEEE International Symposium on*, vol., no., pp.1296-1301, 4-7 July 2010.

[4] M. R. Barzegaran, A. Sarikhani, and O. A. Mohammed, "An equivalent source model for the study of radiated electromagnetic fields in multi-machine electric drive systems," in *proc. IEEE Int. Symp. EMC*, Aug. 14-19, 2011, pp. 442-447

[5] P. Ferrari, A. Mariscotti, and P. Pozzobon, "Electromagnetic emissions from electrical rotating machinery," *IEEE Trans. Energy Convers.,* vol. 16, no. 1, pp. 68-73, Mar. 2001.

[6] F. D. Torre and A. P. Morando, "Study on far-field radiation from three-phase induction machines," *IEEE Trans. Electromagnetic Compatibility,* vol. 51, no. 4, pp. 928-936, Nov. 2009.

[7] A. Rosales, A. Sarikhani and O. A. Mohammed, "Evaluation of radiated electromagnetic field interference due to frequency switching in PWM motor drives by 3D finite elements*," IEEE Trans. Magnetics*, vol.47, no.5, pp. 1474-1477, May 2011.

[8] D. Schneider, M. Beltle, M. Siegel, S. Tenbohlen and W. Kohler, "Radiated Emissions of an Electric Drive System Estimated on a Bench Using Disturbance Currents and Transfer Functions," *IEEE Trans, Electromagnetic compatibility*, vol. 57, no. 3, June 2015.

[9] A. Kriz and W. Milliner, "Analysis of the CISPR 25 component test setup," in Proc. *IEEE Int. Symp. Electromag. Compat*., Boston, MA, Aug. 2003, vol. 1, pp.229-232.

[10] J. Pyrhonen, T. Joinen and V. Hrabovcova., *Design of rotating electrical machines*, 2nd ed. Wiley, 2014.

[11] H. Jo and K. J. Han, "Estimation of Radiation Patters from the Stator Winding of AC Motors Using Array Model," *IEEE Int. Symp. Electromag. Compat*., 2016.

[12] L. Strutzman and G. A. Thiele, *Antenna Theory and Design* 3rd ed., Wiley 2012.

[13] Henry W. Ott, *Electromagnetic Compatibility Engineering*, Wiley, 2009

[14] David M. Pozar, *Microwave Engineering,* 4th ed., New York: Wiley, 2011

Acknowledgement

전자 및 전자공학 분야의 석사과정을 마치고 학위논문을 마무리하게 되었습니다. 아직 갈 길이 멀고 부족하지만, 그동안 많은 도움을 주셨던 분들에게 감사의 말씀을 전하고자 합니다.

총괄적인 연구를 지도해주신 한기진 교수님께 가장 먼저 감사의 표시를 하고 싶습니다. 연구 결과가 조금 부족하지만, 교수님의 섬세하신 지도 덕분에 연구에 흥미를 가지게 되었습니다. 조금 방황했지만, 앞으로 나아갈 길을 지속적으로 응원해 주시면 감사하겠습니다.

갈 곳이 없었던 저희 연구실 분들에게 선처를 베풀어 주셨던 김진국 교수님께도 감사의 표시를 하고 싶습니다. 복잡한 상황속에서 지속적으로 연구를 할 수 있도록 기회를 주시고, 졸업을 준비하는 시기에 여러가지 도움을 주셔서 언제나 감사하고 있습니다. 그리고 바쁘신 와중에도 논문심사를 맡아 주셨던 변강일 교수님께도 감사드립니다.

함께 연구실 생활을 하였던 선배님들께도 감사드립니다. 학회 때 재밌는 인생 얘기를 해주던 영곤이형, 항상 다양한 고민을 잘들어 주시는 만제형, 밤마다 맥주 캔을 꺼내시던 지현누나, 타지에서 고생이 많은 라메쉬, 미안한 일들도 많았지만 석사과정 동안 다사다난한 일들을 모두 함께 고민해주고 도와준 병진이 그리고 자상하게 도움을 주셨던 준식이형을 포함한 김진국 교수님 연구실 학생분들께도 감사인사를 드립니다. 오랜 시간 동안 지속적으로 고민을 따뜻한 조언을 주셨던 민아누나와 화평이형 에게도 감사인사를 드리고 싶습니다.

2012 년 처음 울산에 오게 되어, 7 년이 넘는 시간동안 희로애락을 함께해준 8 명의 12 학번 동기들 주형이, 성식이, 경렬이, 용준이, 상수, 동헌이, 정우, 성경이 에게도 감사 인사를 드립니다. 힘들 때는 커피 한 잔을 건네 주고, 기쁠 때는 맥주 잔을 기울여 주던 친구들이 있었기에, 시간이 지나고나서 생각해보면 모든 순간들이 좋은 추억이 될 것 같아 너무나 행복합니다.

항상 내 편이 되어 응원해주는 가족분들에게 감사 인사를 드리며 글을 마무리하고 싶습니다. 많이 방황을 하던 시기가 있었고, 사실 지금도 많이 부족하지만, 정신적으로 언제나 많은 도움을 받고 있는 저는 정말 행복한 사람인 것 같습니다. 존경하는 부모님과, 힘든 시기를 보내고 있는 형에게 앞으로 행복한 일들만 찾아오고 항상 건강하게 지냈으면 좋겠습니다.